International Journal of Advanced Engineering and Technology Research
ISSN: 3106-8677 (Print), ISSN: 3106-8685 (Online) | Vol. 1, No. 3, 2026

Vision-Based Rebar Diameter Identification via KLT Optical Flow Feature Tracking and Vibration Frequency Inversion

Du Guo

Department of Civil and Environmental Engineering, National University of Singapore, Singapore 117576, Singapore

Abstract: Accurate identification of rebar dimensions is critical for quality control and structural safety in civil engineering. Traditional inspection methods rely on manual measurement or contact-based sensors, which are labor-intensive and inefficient for large-scale or automated applications. This paper presents a vision-based non-contact method for rebar dimension identification by analyzing vibration frequency. The method uses a high-speed camera to capture rebar free vibration, applies the Kanade–Lucas–Tomasi (KLT) algorithm to extract displacement signals, and identifies the dominant frequency via Fast Fourier Transform (FFT). Based on Euler–Bernoulli beam theory, the rebar diameter is then inversely estimated from the identified frequency. Two case studies were conducted for validation. A ruler experiment first confirmed that the KLT-FFT framework can reliably extract vibration frequencies under controlled conditions, with the inversely estimated Young's modulus showing a maximum error of only 2.89%. Subsequent rebar experiments demonstrated that the calculated diameters closely match measured values, verifying the feasibility of frequency-based dimension identification. An additional study on camera motion compensation showed that the method remains robust under in-plane translational disturbances. The proposed approach offers advantages including non-contact operation, low cost, and automation potential, providing a practical basis for rapid rebar dimension assessment in engineering applications.

Keywords: Computer Vision, KLT Algorithm, Vibration Frequency, Rebar Dimension Identification, Euler–Bernoulli Beam Theory, Non-contact Measurement.

1. Introduction

With the advent of automated production and intelligent inspection in modern construction, rapid and efficient identification of rebar dimensions has become increasingly important in civil engineering practice [1]. Dimensional errors in reinforcing bars may lead to construction deviations, reduced structural performance, and even potential safety hazards during installation and service. Traditional contact-based measurement methods, such as vernier calipers, micrometers, and gauges, are simple and accurate for manual inspection; however, they are labor-intensive and inefficient for large-scale or automated applications. As a result, there is a growing demand for non-contact and automated approaches to rebar dimension identification.

Compared with contact-based methods, non-contact approaches, including vision-based measurement, laser measurement, and infrared sensing, provide greater potential for rapid and automated dimensional evaluation. Among them, vision-based methods are particularly attractive because of their low cost, flexible deployment, and compatibility with intelligent inspection systems. Existing vision-based studies on rebar dimension measurement mainly focus on direct geometric extraction from images, such as edge detection, contour extraction, and pixel calibration [2]. These methods have demonstrated the feasibility of non-contact dimensional measurement and provide an efficient alternative to traditional manual inspection. However, their performance often depends heavily on clear geometric boundaries and stable imaging conditions. In practical scenarios, ribbed surfaces, illumination variations, and local contour interference may reduce the robustness and accuracy of direct visual measurement.

To overcome the limitations of direct geometric measurement, vibration-frequency-based dimension inversion has emerged as a promising alternative. Instead of relying on precise extraction of the geometric outline, this approach estimates rebar size indirectly from vibration by identifying dynamic response characteristics, particularly the dominant vibration frequency [3]. Because it depends more on temporal motion information than on clear contour boundaries, it is generally less sensitive to ribbed surfaces, illumination variations, and local disturbances. This provides a complementary pathway for rebar dimension identification in challenging visual environments.

To extract vibration information from image sequences, a range of motion estimation and feature tracking methods have been employed. Optical flow methods are commonly used to describe the apparent motion of image intensity patterns between consecutive frames. Representative methods include Horn–Schunck, Farneback, and Lucas–Kanade optical flow. Among them, dense optical flow methods estimate motion over the entire image, whereas sparse optical flow methods focus on selected feature points or local regions [4]. In parallel, feature-point-based tracking methods are widely used to reconstruct displacement responses from vibrating targets. Common feature detectors include Harris and Shi–Tomasi corner detectors, which are often combined with tracking algorithms to improve robustness.

For small-amplitude and continuous vibration measurement, the combination of the Lucas–Kanade optical flow method and Shi–Tomasi corner detection is particularly suitable. Lucas–Kanade provides efficient local motion estimation, while Shi–Tomasi selects stable and trackable feature points with strong local texture [5]. This combination makes it possible to reconstruct displacement time-history

signals from representative points and to identify dominant vibration frequencies through subsequent frequency-domain analysis.

This study proposes a machine-vision-based method for rebar dimension identification. By capturing vibration videos of rebars, Shi–Tomasi corner detection and Lucas–Kanade optical-flow-based tracking are employed to extract displacement time-history signals from representative feature points[6]. Frequency-domain analysis is then applied to identify the dominant vibration frequency, and the relationship between vibration frequency and rebar geometric parameters is investigated to achieve non-contact dimension identification. The main contributions of this work are as follows:

(i) a machine-vision-based framework for rebar dimension identification is developed by integrating vibration video analysis with frequency-based parameter inversion;

(ii) a combined Lucas–Kanade optical flow and Shi–Tomasi corner detection approach is introduced to extract displacement signals and identify dominant frequency characteristics;

(iii) the feasibility of using vibration frequency as an indicator for rebar dimension identification is experimentally validated through progressive case studies.

2. Theoretical Basis

2.1. Basic Theory of Beam Vibration

The vibration behavior of a beam can be described by the Euler–Bernoulli beam theory, which assumes that the beam is slender, deformation is dominated by bending, and plane sections remain plane and perpendicular to the neutral axis during vibration [6]. Under these assumptions, the transverse free vibration of a uniform beam can be expressed by the following partial differential equation:

$$EI\frac{\partial^4 y(x,t)}{\partial x^4} + \rho A\frac{\partial^2 y(x,t)}{\partial t^2} = 0 \quad (1)$$

Where E is the Young's modulus, I is the second moment of area of the cross-section, ρ is the material density, A is the cross-sectional area, y(x, t) is the transverse displacement, x is the spatial coordinate along the beam axis, and t is time. To solve the free vibration problem, the transverse displacement is commonly written in a separable form y(x, t) = φ(x)q(t), where φ(x) represents the mode shape and q(t) represents the time-dependent response [7].

For a cantilever beam, one end is fixed and the other is free. This boundary condition is consistent with the vibration model used in rebar experiments, where the specimen is clamped at one end and allowed to vibrate freely at the other end after excitation [8]. The general expression for the n-th natural frequency of a uniform Euler–Bernoulli cantilever beam is:

$$f_n = \frac{\beta_n^2}{2\pi L^2}\sqrt{\frac{EI}{\rho A}} \quad (2)$$

Where β_n is the modal coefficient determined by the boundary condition, and L is the effective free length of the beam. For the first-order mode, $\beta_1 \approx 1.875$. Since the first-order vibration mode usually has the largest amplitude and is easiest to capture, it is used as the main frequency feature for structural identification.

2.2. Theoretical Basis for Dimension Identification

The natural frequency of a beam is determined by the balance between its stiffness and mass distribution. The term EI represents bending stiffness, while ρA represents mass per unit length. Changes in cross-sectional area A and second moment of area I directly affect natural frequency [8]. For rebars with circular cross-sections, the geometric parameters can be expressed as $A = \pi d^2/4$ and $I = \pi d^4/64$, where d is the diameter. Substituting into Eq. (2) and simplifying:

$$f_1 = \frac{\beta_1^2}{2\pi L^2}\sqrt{\frac{Ed^2}{16\rho}} \quad (3)$$

This result shows that, under the assumption of constant material properties and fixed boundary conditions, the natural frequency is closely related to the diameter of the rebar. Rearranging the above equation, the diameter can be expressed as:

$$d = \frac{8\pi f L^2}{\beta_1^2}\sqrt{\frac{\rho}{E}} \quad (4)$$

This equation indicates that when the material density, Young's modulus, modal coefficient, and effective free length are known, the rebar diameter has an explicit functional relationship with its natural frequency. In practical applications, commonly used rebars are made of similar steel materials, and the variations in density and Young's modulus are usually relatively small. By contrast, changes in diameter have a more significant influence on cross-sectional area and bending stiffness [9]. Therefore, the frequency differences caused by dimension variations are often distinguishable, and the diameter can be inversely estimated from the measured vibration frequency.

3. Proposed Methodology

The proposed vision-based frequency identification approach consists of four main stages: video acquisition and ROI definition, feature detection and tracking, displacement signal reconstruction and frequency identification, and frequency-based diameter estimation. This section describes each stage in detail.

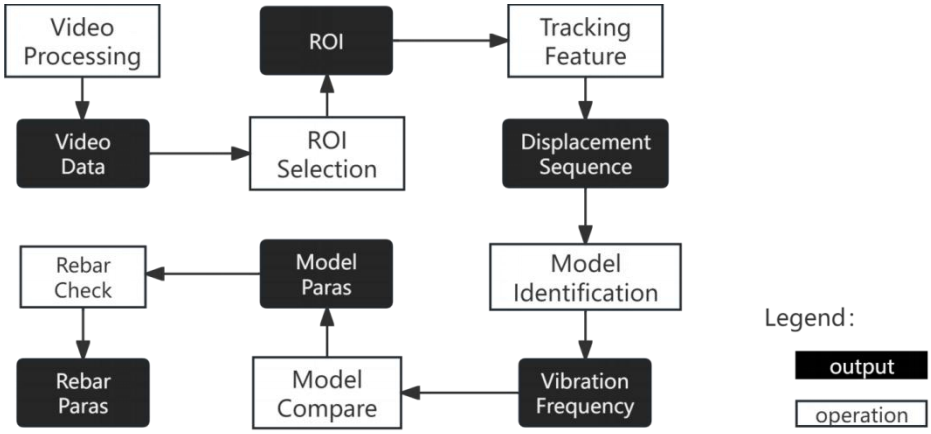

Figure 1. Workflow of the proposed vision-based frequency identification method

3.1. Video Acquisition and ROI Definition

The first step is to acquire vibration videos of the rebar under excitation. A camera records the free-vibration response after excitation, requiring a sufficiently high frame rate and clear image resolution [10]. The camera should be positioned perpendicular to the vibrating segment to reduce perspective distortion, and the shooting distance should be adjusted so that the rebar occupies sufficient pixels for feature extraction while the entire vibrating segment remains within the field of view. Stable illumination is preferred, while strong reflections, shadows, and excessive background interference should be avoided [11].

After video acquisition, a Region of Interest (ROI) is defined to isolate the effective vibrating part of the rebar from the surrounding background. The ROI should fully cover the vibrating segment during the entire motion process and contain sufficient texture or artificial markers for stable feature tracking. At the same time, irrelevant regions should be excluded to reduce noise interference and improve computational efficiency.

3.2. Shi–Tomasi Corner Detection

The Shi–Tomasi corner detector is used to identify feature points suitable for reliable tracking. For the grayscale ROI image, the horizontal and vertical image gradients are first computed, and the local structure tensor M is constructed. Unlike the Harris detector, which uses a combined determinant-trace response function, the Shi–Tomasi method directly evaluates the minimum eigenvalue of the structure tensor as the corner response [12]:

$$R(x,y) = \min(\lambda_1, \lambda_2) \tag{5}$$

Where λ_1 and λ_2 are the two eigenvalues of M. A pixel is selected as a candidate feature point if R(x,y) exceeds a predefined threshold, ensuring that the point exhibits strong intensity variation in all directions and is thus reliably trackable. After thresholding and non-maximum suppression, the final set of feature points is obtained.

3.3. KLT-Based Feature Tracking

After initial feature points are detected, the Kanade–Lucas–Tomasi (KLT) algorithm tracks their motion in consecutive image frames. The KLT algorithm is based on the brightness constancy assumption, which states that the grayscale value of the same image point remains approximately unchanged over a short time interval [13]. By applying first-order Taylor expansion, the optical flow constraint equation can be written as:

$$I_x u + I_y v + I_t = 0 \tag{6}$$

Where u and v denote the motion components in the image plane. Since the motion of a single pixel cannot be uniquely solved, the KLT algorithm estimates the displacement of each feature point within a local neighborhood by weighted least squares. The purpose of KLT tracking is to obtain reliable time-history motion signals from representative points on the vibrating rebar, rather than to reconstruct the full-field displacement [14].

Not all detected feature points are equally suitable for vibration analysis. Some may suffer from tracking drift, temporary loss, weak texture, or noise contamination. Therefore, an additional selection step retains only reliable points that can be tracked continuously, are located on the rebar surface, and exhibit smooth periodic trajectories. If multiple reliable points are retained, their displacement trajectories can be averaged to improve robustness and reduce random noise.

3.4. Displacement Signal Reconstruction and Frequency Identification

Once the trajectories of reliable feature points are obtained, the vibration response is reconstructed as a discrete displacement time-history signal x[n], n = 0, 1, ..., N-1. Before frequency analysis, the signal is preprocessed by removing the mean value or slow-varying trends to reduce low-frequency interference unrelated to structural vibration [15].

The Fast Fourier Transform (FFT) is then applied to transform the displacement signal from the time domain to the frequency domain:

$$X[k] = \sum_{n=0}^{N-1} x[n]\, e^{-j2\pi kn/N}, k = 0,1,\ldots,N-1 \tag{7}$$

The frequency resolution is $\Delta f = f_s/N$, and the dominant vibration frequency is identified from the main spectral peak. It should be noted that dominant frequency identification mainly depends on the periodicity of the signal rather than its absolute amplitude. Therefore, pixel-level displacement can be directly used for FFT-based frequency analysis without conversion to physical units [16].

3.5. Frequency-Based Diameter Estimation

The dominant vibration frequency extracted from the video signal provides the basis for rebar diameter identification. By combining the identified dominant frequency with the theoretical frequency–diameter relationship established in Eq. (4), the diameter can be estimated indirectly. Under standardized testing conditions, rebars with different

diameters can be distinguished based on their frequency features. In practical applications, the identified frequency may be compared with theoretical predictions, calibration results, or pre-established frequency–diameter mappings.

4. Experimental Validation and Case Studies

This chapter validates the proposed vision-based frequency identification method through three progressive case studies. Each serves a distinct purpose: Case Study I verifies the KLT-FFT framework using a ruler with known properties; Case Study II investigates rebar dimension identification on actual engineering specimens; and Case Study III evaluates robustness under camera motion. Together, these form a complete validation chain from basic verification to practical application to complex scenario extension [17].

Table 1. Overview of experimental case studies

Case	Specimen	Camera	Sample Size	Objective
I	Ruler	Static	6 tests	Method validation
II	Rebar	Static	27 tests	Dimension identification
III	Rebar	Moving	3 tests	Robustness evaluation

4.1. Case Study I: Method Validation Using Ruler Specimen

A ruler specimen with known geometric and material properties was used to validate the correctness of the proposed framework. The ruler (total length 61 cm, cross-sectional area 1.32 cm^2, second moment of area 9.691×10^{-3} cm^4, density 1.1798 g/cm^3) was configured as a cantilever beam. Video was recorded at 4K resolution and 120 fps using an iPhone mounted on a tripod. The camera was positioned perpendicular to the ruler to reduce perspective distortion.

The effective free length was varied across six levels by adjusting the fixation position at marks of 0.5, 9, 12, 13, 15, and 21 cm, yielding effective lengths of 60.0, 51.5, 48.5, 47.5, 45.5, and 39.5 cm respectively. For each test condition, the experiment was repeated to ensure data reliability. The free end of the ruler was lightly tapped by hand to trigger free vibration, and the most stable 10-second segment was selected for analysis.

After ROI selection, feature points were detected using Harris corner detection and tracked using the KLT algorithm. The tracked pixel displacements were used to reconstruct the vibration response, with multiple feature point trajectories averaged to reduce random fluctuation. FFT was then applied to identify the dominant frequency.

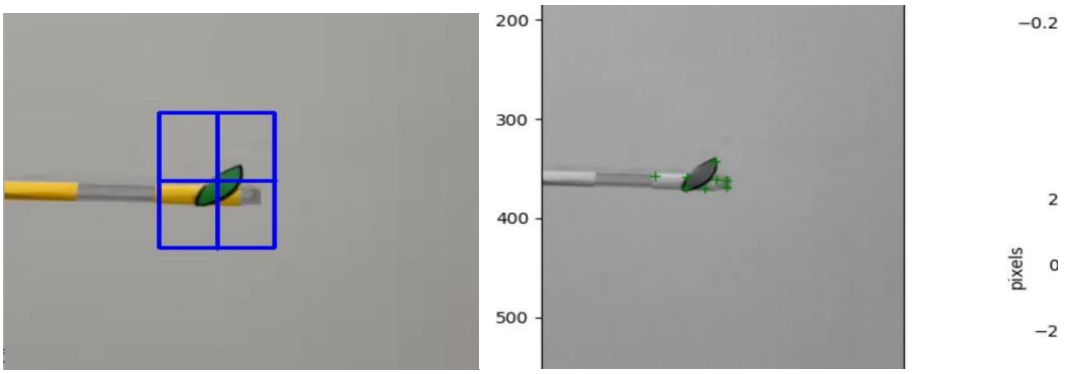

Figure 2. ROI selection for ruler specimen

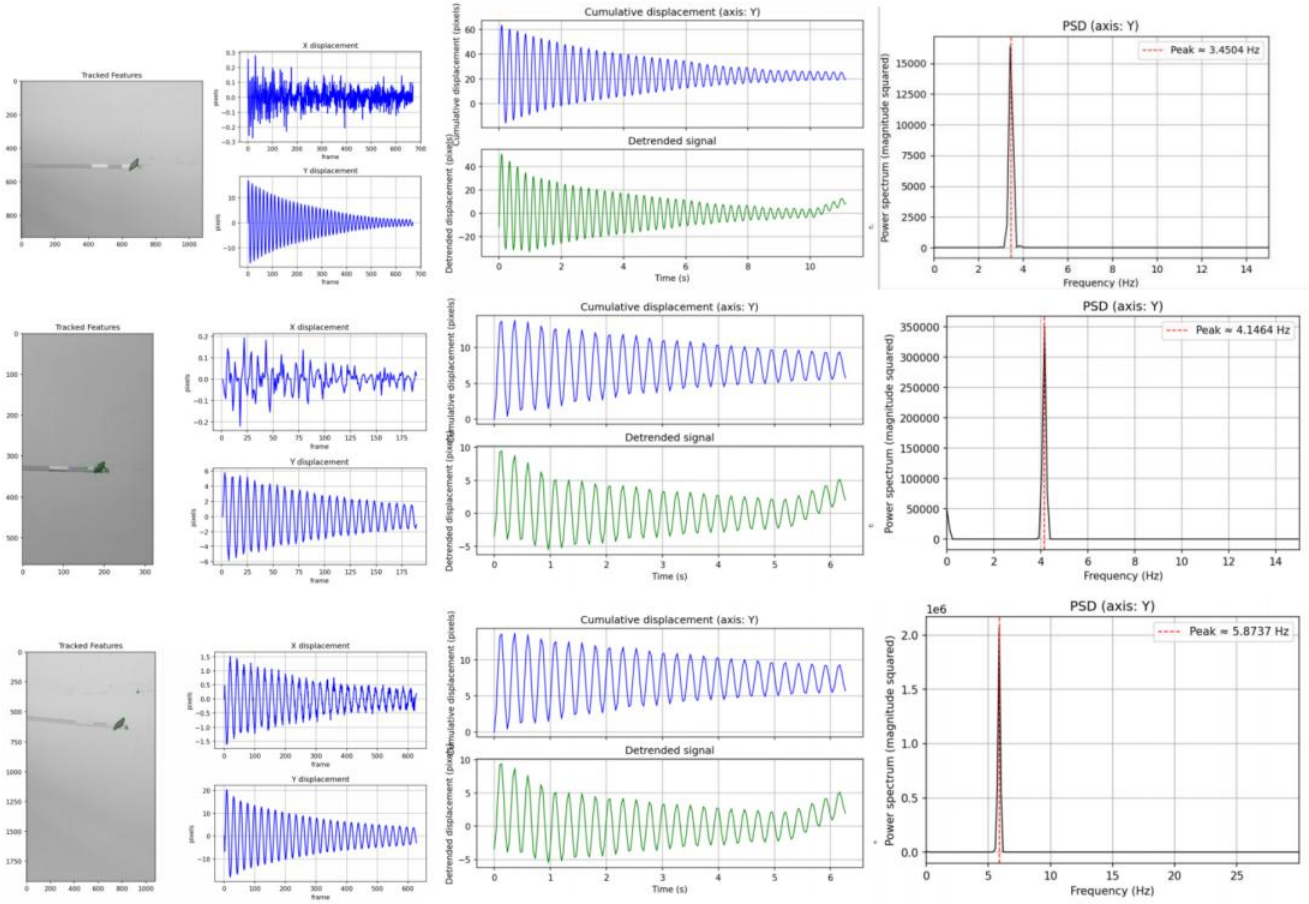

Figure 3. Examples of vibration signal extraction from ruler

To verify the consistency of the proposed method, the inversely estimated Young's modulus was calculated from the identified frequencies using the Euler–Bernoulli cantilever beam model:

$$E = \frac{(2\pi f_n L^2)^2 \rho A}{\beta_n^4 I} \quad (8)$$

Since all measurements were performed on the same ruler, the estimated values should remain close if the method is stable. Results are shown in Table 2.

Table 2. Identified frequencies and estimated Young's modulus for ruler specimen

L (cm)	Frequency (Hz)	E (GPa)	Error (%)
60.0	2.573	4.402	0.94
51.5	3.477	4.366	0.11
48.5	3.924	4.373	0.27
47.5	4.140	4.479	2.71
45.5	4.388	4.235	2.89
39.5	5.876	4.315	1.05

As shown in Table 2, the estimated Young's modulus values under different test conditions remain within a relatively narrow range, with a maximum deviation of 2.89% from the mean estimated value. This confirms that the dominant frequencies identified from different recordings are highly consistent [18]. The results also show a clear trend between effective free length and dominant frequency: as the effective free length decreases, the identified natural frequency increases accordingly. This trend is consistent with beam vibration theory and confirms that the method correctly reflects the dynamic behavior of the specimen.

The successful validation in this controlled experiment establishes confidence in applying the method to actual rebar specimens [19]. The estimated Young's modulus consistency demonstrates that the KLT-FFT framework can reliably extract frequency features, which is essential for subsequent dimension identification tasks.

4.2. Case Study II: Rebar Dimension Identification

Building on the validated framework, this case study investigates whether vibration frequency can serve as an effective indicator for rebar dimension classification. Seven rebar specimens with known dimensions were prepared for testing. The specimens include different diameters (6–12 mm) and lengths (156–320 cm), with both deformed and plain bars. Artificial feature points were marked on the rebar surface to improve motion feature visibility.

Figure 4. Rebar specimens used in Case Study II

Table 3. Information of rebar specimens

Rebar ID	Length (cm)	Diameter Range (cm)	Description
1	156	0.6–0.7	Deformed bar
2	200	1.1–1.2	Deformed bar No.1
3	200	1.1–1.2	Deformed bar No.2
4	200	1.1–1.2	Deformed bar No.3
5	200	1.1–1.2	Deformed bar No.4
6	320	1.1–1.2	Deformed bar
7	217	1.0–1.1	Plain bar

Each rebar specimen was rigidly fixed to a support frame to form a cantilever beam configuration. A white background board was placed behind the specimen to enhance image contrast. Controlled excitation was applied to the free end using an impact hammer to induce free vibration [20]. The same video acquisition system (4K, 120 fps) was used, and each experiment was repeated three times.

Figure 5. Schematic diagram of rebar fixation

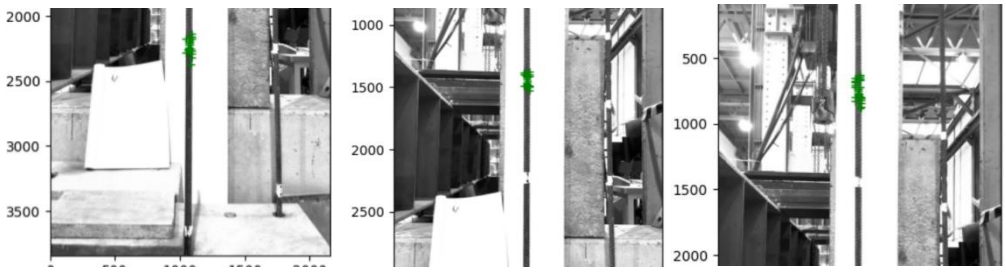

Figure 6. Feature point detection and tracking for rebars

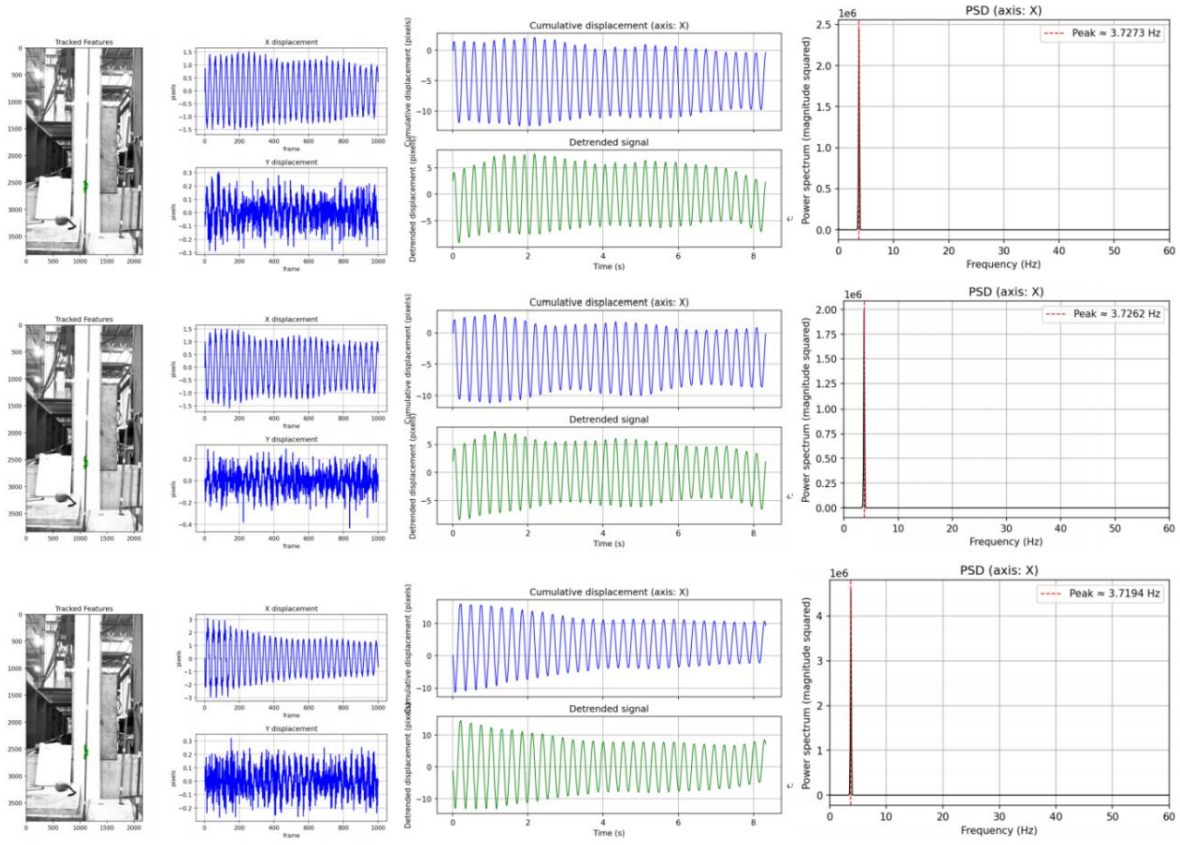

Figure 7. Examples of extracted vibration signals from rebars

Material properties were assumed as $\rho = 7850\ kg/m^3$ and $E = 200\ GPa$ for all steel rebars. The captured videos were preprocessed with denoising, grayscale conversion, and ROI selection [21]. Harris corner detection identified feature

points, which were tracked by the KLT algorithm. The dominant frequencies were extracted via FFT and used to calculate diameters using Eq. (4). The formula for calculating cross-sectional area from frequency is:

$$A = \frac{16\pi^3 \rho L^4 f_1^2}{\beta_1^4 E} \quad (9)$$

The diameter is then obtained from $d = \sqrt{(4A/\pi)}$. Representative results comparing calculated and measured diameters are shown in Table 4.

Table 4. Calculated diameter vs. measured diameter of rebar specimens

Rebar ID	L (cm)	Mean Freq. (Hz)	Calc. Diam. (cm)	Measured (cm)	Nominal
1	107	3.728	0.604	0.6–0.7	6 mm
2	151	3.252	1.050	1.0–1.1	10 mm
3	151	3.237	1.045	1.0–1.1	10 mm
4	151	3.213	1.016	1.0–1.1	10 mm
5	151	3.231	1.044	1.0–1.1	10 mm
6	271	1.052	1.095	1.0–1.1	10 mm
7	168	2.672	1.068	1.0–1.1	10 mm

The results show that the identified dominant frequencies vary with the geometric parameters of the specimens. For Rebar 1, the three calculated diameters are 0.6044, 0.6042, and 0.6047 cm, which agree well with the measured range of 0.6–0.7 cm. For Rebars 2–5, which share similar dimensions (200 cm length, 1.1–1.2 cm diameter), the mean calculated diameters cluster around 1.0–1.05 cm, consistent with the measured range. For Rebar 6 (the longest specimen at 320 cm), the five calculated diameters range from 1.073 to 1.119 cm. For Rebar 7 (the plain bar), the mean calculated diameter is 1.068 cm, also within the measured range.

These results indicate that, under standardized testing conditions, the cross-sectional parameters inversely estimated from vibration frequency can reasonably reflect the actual dimensional level of the tested rebars [22]. The mean calculated diameter can be used to determine the nominal diameter class of each specimen [23]. Specimens with similar effective lengths exhibit distinguishable frequency variations corresponding to diameter differences, confirming the potential of frequency-based dimension classification.

4.3. Case Study III: Frequency Identification under Camera Motion

In practical engineering scenarios, maintaining a perfectly static camera during video acquisition is often difficult. Camera motion may introduce additional disturbance into the extracted vibration signal, affecting frequency identification accuracy [24]. This case study evaluates the method's robustness under handheld-camera conditions by introducing three types of controlled camera motion: horizontal, vertical, and forward–backward.

(a) Reference ROI (b) Object ROI

Figure 8. Reference and object ROIs used for motion compensation

A motion-compensation strategy using dual ROIs is incorporated. A static Reference ROI on the background captures camera-induced motion, and an Object ROI covers the vibrating target. The camera-induced displacement is approximated by the reference motion:

$$\Delta \mathbf{c}(k) \approx \Delta \mathbf{r}(k) \quad (10)$$

The compensated relative displacement of the target is obtained by subtracting reference motion from object motion:

$$\Delta \mathbf{u}(k) = \Delta \mathbf{o}(k) - \Delta \mathbf{r}(k) \quad (11)$$

The cumulative compensated displacement $u(k) = \Sigma \Delta u(m)$ is then transformed into the frequency domain for dominant frequency identification.

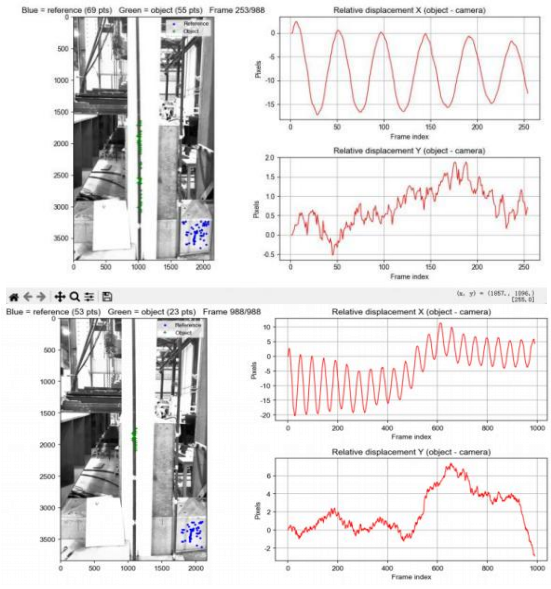

Figure 9. Schematic diagram of motion compensation process

Results show that when the camera motion remains within

the ROI, the compensation method performs differently under different motion types [25]. For horizontal and vertical camera motions, compensated signals still exhibit clear periodicity, and the identified dominant frequencies are close to those obtained under static-camera conditions [26]. This indicates that the method can effectively suppress in-plane translational disturbances and stably extract the true vibration response.

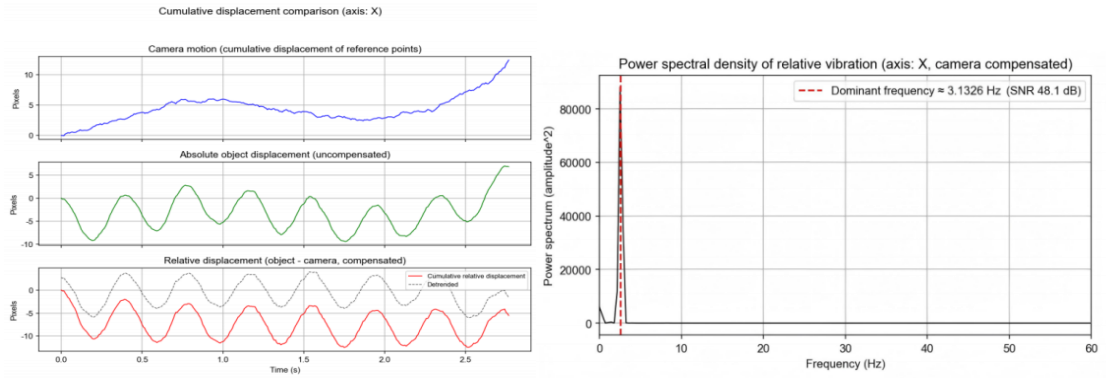

(a) Results under horizontal camera motion

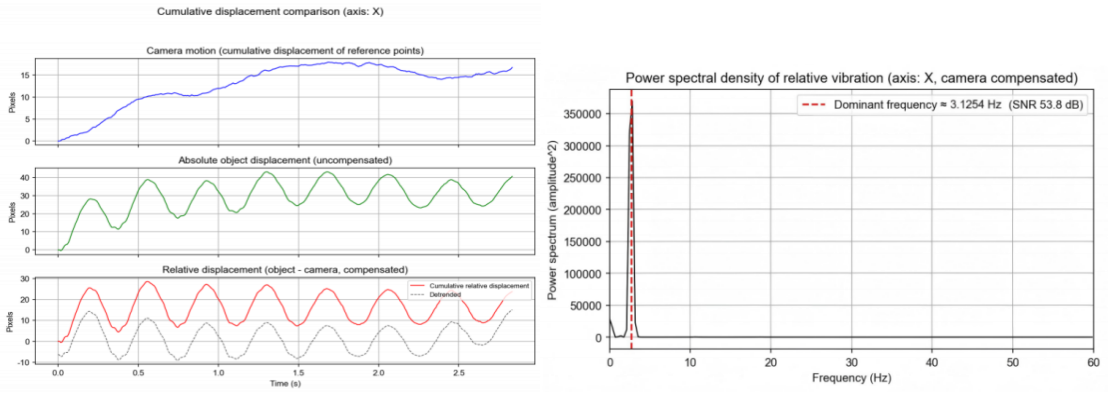

(b) Results under vertical camera motion

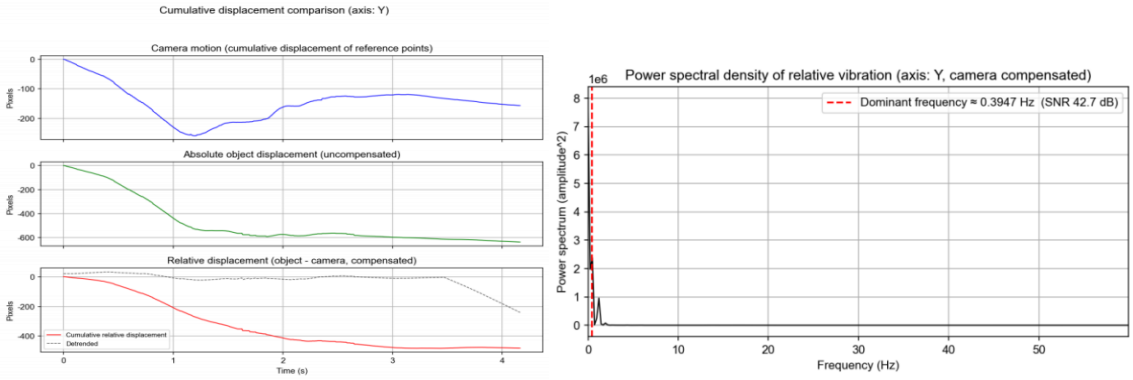

(c) Results under forward–backward camera motion

Figure 10. Extracted vibration signals under diferent camera motion conditions

In contrast, under forward–backward camera motion, the compensated signal fails to preserve correct vibration characteristics, and the identified frequency deviates significantly from the true value. This is because forward–backward motion introduces scale variation and perspective effects that cannot be fully removed by the current displacement-differencing strategy [27]. Overall, the method is robust for in-plane translational disturbances but requires further development for optical-axis movements.

5. Conclusions

This paper investigated a vision-based non-contact method for rebar dimensional assessment based on vibration-frequency identification. A complete technical framework was established integrating video acquisition, ROI definition, KLT-based feature tracking, FFT-based frequency identification, and Euler–Bernoulli beam theory for diameter estimation.

A preliminary experiment using a ruler specimen validated the feasibility of the proposed method. The vision-based framework stably captured vibration responses and repeatedly identified dominant frequencies under different effective free lengths, with the inversely estimated Young's modulus showing a maximum error of only 2.89%. The clear inverse relationship between length and frequency is consistent with beam vibration theory, confirming the correctness of the technical route.

Experiments on actual rebar specimens further demonstrated that the proposed method can stably extract vibration responses and identify dominant frequencies from video data. The diameters inversely estimated from the identified frequencies are generally close to measured values,

confirming the feasibility of using vibration frequency as a characteristic feature for rebar dimension identification under standardized conditions.

The camera motion compensation study showed that the dual-ROI strategy effectively suppresses in-plane translational disturbances, while forward–backward motion remains a limitation due to perspective effects.

Compared with traditional contact-based methods, the proposed approach is non-contact, low-cost, easy to deploy, and potentially suitable for automated inspection. Since it relies on vibration-response characteristics rather than direct contour extraction, it provides an alternative pathway for dimension assessment when geometric boundaries are unclear.

The present work has some limitations. The experiments were conducted mainly under controlled laboratory conditions, and the number of tested specimens was limited. The identified vibration frequency is influenced by boundary conditions, effective free length, excitation consistency, and material properties, requiring relatively standardized testing conditions for reliable identification.

Future work can be extended in several directions: establishing a comprehensive frequency–dimension database using rebars of different sizes and conditions; introducing more robust feature extraction and tracking algorithms for varying field environments; developing statistical or learning-based identification models combining theoretical analysis with data-driven calibration; and integrating the method with automated sorting, robotic grasping, and intelligent inspection systems for practical deployment in civil engineering.

References

[1] Pan, B. Digital image correlation for surface deformation measurement: historical developments, recent advances and future goals. Measurement Science and Technology, 29(8) (2018), 082001.

[2] Brownjohn, J. M. W. Structural health monitoring of civil infrastructure. Philosophical Transactions of the Royal Society A, 365 (2007), 589–622.

[3] Ye, X. W., Dong, C. Z., Liu, T. A review of machine vision-based structural health monitoring: Methodologies and applications. Journal of Sensors, 2016 (2016), 7103039.

[4] Xu, Y., Brownjohn, J. M. W. Review of machine-vision based methodologies for displacement measurement in civil structures. Journal of Civil Structural Health Monitoring, 8 (2018), 91–110.

[5] Feng, D., Feng, M. Q., Ozer, E., Fukuda, Y. A vision-based sensor for noncontact structural displacement measurement. Sensors, 15 (2015), 16557–16575.

[6] Khuc, T., Catbas, F. N. Completely contactless structural health monitoring of real-life structures using cameras and computer vision. Structural Control and Health Monitoring, 24 (2017), e1852.

[7] Morlier, J., Michon, G. Virtual vibration measurement using KLT motion tracking algorithm. Journal of Dynamic Systems, Measurement, and Control, 132(1) (2010), 011003.

[8] Pan, B., Qian, K., Xie, H., Asundi, A. Two-dimensional digital image correlation for in-plane displacement and strain measurement: A review. Measurement Science and Technology, 20 (2009), 062001.

[9] Dong, C. Z., Catbas, F. N. A review of computer vision-based structural health monitoring at local and global levels. Structural Health Monitoring, 20(2) (2021), 692–743.

[10] Lee, J. J., Shinozuka, M. A vision-based system for remote sensing of bridge displacement. NDT & E International, 39(5) (2006), 425–431.

[11] Guo, J., Zhu, C. Dynamic displacement measurement of large-scale structures based on the Lucas–Kanade template tracking algorithm. Mechanical Systems and Signal Processing, 66–67 (2016), 425–436.

[12] Baker, S., Matthews, I. Lucas-Kanade 20 years on: A unifying framework. International Journal of Computer Vision, 56(3) (2004), 221–255.

[13] Spencer, B. F., Hoskere, V., Narazaki, Y. Advances in computer vision-based civil infrastructure inspection and monitoring. Engineering, 5 (2019), 199–222.

[14] Hoskere, V., Park, J. W., Yoon, H., Spencer, B. F. Vision-based modal survey of civil infrastructure using unmanned aerial vehicles. Journal of Structural Engineering, 145 (2019), 04019062.

[15] Shi, J., Tomasi, C. Good features to track. In: Proceedings of the IEEE Conference on Computer Vision and Pattern Recognition (1994), 593–600.

[16] Morlier, J., Michon, G. Virtual vibration measurement using KLT motion tracking algorithm. Journal of Dynamic Systems, Measurement, and Control, 132(1) (2010), 011003.

[17] Yoon, H., Elanwar, H., Choi, H., Golparvar-Fard, M., Spencer, B. F. Target-free approach for vision-based structural system identification using consumer-grade cameras. Structural Control and Health Monitoring, 23 (2016), 1405–1416.

[18] Rao, S. S. Mechanical Vibrations. 5th ed. Pearson, 2011.

[19] Chopra, A. K. Dynamics of Structures: Theory and Applications to Earthquake Engineering. 4th ed. Pearson, 2012.

[20] Yin, A., Yu, Q., Zhang, Q., Ma, S. Optical flow tracking method for vibration identification of out-of-plane vision. Journal of Vibroengineering, 19(4) (2017), 2363–2374.

[21] Blevins, R. D. Formulas for Natural Frequency and Mode Shape. Krieger Publishing, 2001.

[22] Dong, C. Z., Catbas, F. N. A review of computer vision-based structural health monitoring at local and global levels. Structural Health Monitoring, 20(2) (2021), 692–743.

[23] Nikoo, M., Hadzima-Nyarko, M., Khademi, F., Mohasseb, S. Estimation of fundamental period of reinforced concrete shear wall buildings using self organization feature map. Structural Engineering and Mechanics, 63(2) (2017), 237–249.

[24] Pan, B. Reliability-guided digital image correlation for image deformation measurement. Applied Optics, 48 (2009), 1535–1542.

[25] Kim, S. W., Kim, N. S. Dynamic characteristics of suspension bridge hanger cables using digital image processing. NDT & E International, 59 (2013), 25–33.

[26] Lucas, B. D., Kanade, T. An iterative image registration technique with an application to stereo vision. In: Proceedings of the 7th International Joint Conference on Artificial Intelligence (1981), 674–679.

[27] Bouguet, J. Y. Pyramidal implementation of the Lucas-Kanade feature tracker: Description of the algorithm. Intel Corporation, Microprocessor Research Labs, Technical Report, 2001.